Available online at www.sciencedirect.com
ScienceDirect
Combustion and Flame 154 (2008) 23–46
Combustion and Flame
www.elsevier.com/locate/combustflame

One-dimensional turbulence-based closure with extinction and reignition

Bhargav Ranganath, Tarek Echekki *

Department of Mechanical and Aerospace Engineering, North Carolina State University, Raleigh, NC 27695-7910, USA

Received 26 April 2007; received in revised form 15 January 2008; accepted 15 January 2008

Available online 19 May 2008

Abstract

Scalar statistics from stand-alone one-dimensional turbulence (ODT) simulations are constructed to develop a doubly conditioned table based on the mixture fraction and temperature for the prediction of extinction and reignition in piloted methane–air jet diffusion flames. The ODT-based closure approach is formulated to predict scalar statistics coupled with the Reynolds-averaged Navier–Stokes (RANS) approach. Comparison with experimental correlations of reactive scalars with the two conditioning variables show that double conditioning may be adequate to prescribe scalar statistics in the jet diffusion flames. The results also show that the ODT model may be used to construct these statistics. The 2D conditioning table is coupled with RANS to compute Sandia flames D, E, and F, which exhibit increasing rates of extinction followed by reignition as the Reynolds numbers are increased. The coupling also requires the transport of the means and variances of the mixture fraction and temperature. Closure terms in the temperature mean and variance equations are obtained by using the 2D table for reaction source terms and by assuming a presumed PDF shape for the temperature PDF. Comparisons show adequate predictions of axial and radial profiles of the mixture fraction, the streamwise velocity, and the reactive scalars for flames D and E and mixed results for flame F. Nonetheless, qualitative trends of increasing the jet Reynolds numbers resulting in more pronounced extinctions are obtained with the RANS-ODT approach. The discrepancy between computation and experiment may be attributed primarily to the closure for the temperature and its variance and to the presumed PDF shape for the temperature.

Keywords: ODT-based closure; Extinction and reignition; Turbulent nonpremixed combustion; Piloted jet diffusion flames

1. Introduction

The prediction of extinction and reignition in turbulent flames has recently evolved into an important target for the validation of state-of-the-art turbulent combustion models. These models can generally be classified into two main classes: moment methods and probability density function approaches [1]. Among the more advanced turbulent combustion modeling approaches based on moment methods, we cite the flamelet approach [2] and the conditional moment closure (CMC) model [3]. In nonpremixed flames, and in their simplest formulation, a reduced-space approach is adopted for the solution of reactive scalars and their associated source terms based on the transport of a passive scalar, the mixture fraction, and its variance. The transport of these two lower mo-

* Corresponding author. Fax: +1 919 515 7968.
E-mail address: techekk@eos.ncsu.edu (T. Echekki).

0010-2180/$ – see front matter
doi:10.1016/j.combustflame.2008.03.020

ments makes possible the construction of reactive scalar statistics based on an assumed shape probability density function (PDF) and the parameterization of the flame response. While the strategies adopted in both the flamelet model and the CMC approaches enabled the implementation of detailed chemistry coupled with transport in turbulent combustion, their extension to transient combustion problems, such as extinction and reignition processes, requires additional refinements.

An assessment of the physical predictions of models based on moment methods must be addressed from the perspective of three common components of these models. The first component is related to the model's ability to reasonably span the reduced space (e.g., mixture fraction, dissipation rates, temperature) and predict reactive scalar statistics accurately in this space. The second critical component is the construction of statistics of these scalars; in this regard, the traditional strategy is to use a presumed shape for the joint scalar PDF. However, these PDFs are relatively more complex when the transported scalars are subject to both chemistry and mixing. The third component is related to the development of robust closure formulations for transport and source terms for the transported moments. In this regard, the task is more difficult for higher moments (e.g., mixture fraction variance, dissipation rate) and reactive scalars (e.g., temperature, sensible enthalpy).

The challenges associated with the three components just cited are clearly evident in the prediction of extinction and reignition in nonpremixed flames. The choice of a single reduced-space parameter, the mixture fraction, is not sufficient to predict the process. Sripakagorn et al. [4] identified three major scenarios for reignition in nonpremixed mixtures: (1) the independent flamelet scenario, (2) reignition via edge (triple) flame propagation, and (3) reignition through engulfment by a hot neighborhood. The second and third mechanisms may not be prescribed using the mixture fraction alone [5–9]. Recent studies with CMC (see for example [7,8]) have shown that the use of double conditioning results in better predictions of the nonequilibrium effects associated with highly turbulent flames such as the flames considered in the present work. Similar observations were made using the flamelet model, based on the transport of a passive scalar and a reactive scalar (see for example [9]).

The recent work by Kronenberg and Kostka [8] provides the first extension of the CMC approach with multiple conditioning to address extinction and reignition in the Sandia piloted flames D, E, and F [10]. These flames are characterized by increased rates of extinction followed by reignition as the jet velocities are increased. The model is based on a precomputed parameterized reference field based on two conditioning parameters: the mixture fraction and the sensible enthalpy. The implementation of the model of Kronenberg and Kostka [8] to predict extinction and reignition in flames D, E, and F shows increasing trends of extinction followed by reignition as the jet Reynolds number is increased. While the qualitative trends of the experimental data are reproduced, important discrepancies between experimental and computed scalar statistics are present even under intermediate flame conditions (flame E). A principal constraint on the prediction of flames E and F is associated with the choice of the presumed PDF shape for the sensible enthalpy (the second important component of moment methods). Again, experimental observations by Barlow and Frank [10] have already established important transitions in reactive scalar conditional PDFs during the extinction and reignition process. The study by Kronenberg and Kostka [8] also include closure for the transport equations for the sensible enthalpy and its variance; this closure also involves additional assumptions about transport and source terms in these equations. Similar constraints have been recognized in other moment-based approaches to the modeling of extinction and reignition, such as the recent study by Ihme et al. [9], which is based on a flamelet/progress variable approach.

The linear-eddy model (LEM) [11–13] and the one-dimensional turbulence (ODT) model [14] represent an alternative strategy to account for finite-rate chemistry effects in turbulent combustion. The LEM is a one-dimensional mixing model that incorporates molecular processes (with structure) in a deterministic way, through solutions of 1D unsteady reaction–diffusion equations, and turbulent stirring stochastically through "triplet maps." A more recent refinement of the LEM approach is the ODT model. In contrast with LEM, a mixing model, ODT is a turbulence model. In ODT, one or more components of the velocity vector are transported. Therefore, the ODT model enables a mechanism for "driving turbulence." The frequency and the eddy size distribution are determined by the local flow field. The LEM and ODT models may be implemented as standalone models for turbulent flows where a dominant direction of the flow may be identified *a priori*.

Both LEM and ODT have been implemented as standalone models to predict extinction and reignition [15–18]. Goldin and Raman [16] constructed joint PDFs of species and temperature from a simplified stationary isotropic turbulence solution using the LEM. The constructed PDFs were applied to the prediction of scalar statistics in the Sandia piloted flames D and F. Comparison with experimental data yields excellent agreement and predictions of the processes of extinction and reignition. Hewson and Ker-

stein [17] applied the ODT model to the study of turbulent $CO/H_2/N_2$ flames. Their simulations demonstrated the ODT predictions of extinction and reignition. A follow-up study by the same authors [18] investigated the mechanisms of extinction and reignition in similar flames, but using a wider range of Reynolds numbers and the role of mixing in determining these processes.

Within the context of ODT coupled with a 3D approach, we cite the recent work by the present authors [19]. The authors performed standalone simulations of ODT of turbulent nonpremixed hydrogen flames, which were implemented in the same manner as Echekki et al. [20]. ODT statistics of scalars and temperature based on two parameters, which measure the extent of mixing and entrainment, were tabulated and looked up using Reynolds-averaged Navier–Stokes (RANS) simulation of the same jet. The resulting formulation yields reasonably good agreement with experimental data from hydrogen–air jet diffusion flames [19].

In the present study, we implement the ODT model within the context of a moment method, where scalar statistics are represented in terms of a reduced variable space, conditioned upon the mixture fraction and temperature, to establish whether a reduced space representation based on 2D conditioning is adequate to represent the process of extinction and reignition. An important outcome within this scope is that ODT can adequately map the reduced space and represent scalar statistics. If true, ODT would represent an alternative to strategies based on increasing the dimensions of the reduced space either through the solution for higher moments or through additional conditioning variables. Therefore, a principal aim of the present study is to show that ODT can address the first critical component of modeling based on moment methods, which is associated with the prediction of reactive scalars in terms of a reduced parameter space. The second aim is to couple the ODT-based reduced space description of extinction and reignition to model Sandia flames D, E and F. Although potential limitations of the governing equations for means and variances of temperature and in the use of a presumed PDF shape are recognized, the principal aim here is to develop an alternative strategy to represent extinction and reignition in nonpremixed flames. The additional components of the model will be addressed with "standard" approaches involving transport equations for the mean temperature and its variance and a presumed shape for the joint PDF of temperature and mixture fraction.

Therefore, among the main objectives of the present work are the following: (1) to validate whether the use of a reduced variable set is adequate for the prediction of scalar statistics in piloted methane jet diffusion flames, (2) to assess whether ODT simulations are able to reproduce these statistics, and (3) to use the statistics tabulated based on the reduced variable set, coupled with components 2 and 3 of moment methods to predict spatial statistics of these flames.

2. Model formulation

2.1. General strategy

The present formulation is based on two separate sets of simulations: (a) stand-alone ODT simulations of piloted methane–air jet diffusion flames, and (b) RANS simulations of the same jet flame configuration for flames D, E, and F. The ODT simulations are designed to adequately span the reduced space represented by the mixture fraction and temperature and adequately represent reactive scalars' statistics through double conditioning with respect to the reduced space parameters. Transport equations for the means and variances of the mixture fraction and temperature are solved along with equations for mass and momentum transport and turbulence closure in the RANS simulations. The key closure contributions to these equations are obtained from the 2D table from ODT and assumptions about their PDF; these contributions include primarily closure for the mean density and the source terms in the equations for temperature and its variance in RANS.

2.2. ODT formulation, run conditions, and 2D table generation

The configuration adopted for the simulation of the piloted jet diffusion flames is similar to the one already implemented by Echekki et al. [20]. The formulation is implemented for a temporally evolving planar jet. Deterministic and stochastic solutions are implemented concurrently within the jet simulations. Turbulent transport is implemented stochastically through stirring events or triplet maps. Molecular processes, including chemistry and diffusive transport, are implemented deterministically through solutions of unsteady transport equations for the streamwise velocity component and thermochemical scalars, the species mass fractions and the temperature [20]. The governing equations are as follows:

- streamwise momentum,

$$\frac{\partial u}{\partial t} = \frac{1}{\rho}\frac{\partial}{\partial y}\left(\mu\frac{\partial u}{\partial y}\right), \tag{1}$$

- species,

$$\frac{\partial Y_\alpha}{\partial t} = -\frac{1}{\rho}\frac{\partial}{\partial y}(\rho V_\alpha Y_\alpha) + \frac{\dot{\omega}_\alpha}{\rho}, \tag{2}$$

- temperature,

$$\frac{\partial T}{\partial t} = \frac{1}{\rho \bar{c}_p} \sum_{k=1}^{N} c_{p,k} Y_k V_k \frac{\partial T}{\partial y} + \frac{1}{\rho \bar{c}_p} \frac{\partial}{\partial y} \left(\lambda \frac{\partial T}{\partial y} \right) - \frac{\dot{\omega}_T}{\rho}. \quad (3)$$

The spatial coordinate, y, corresponds to the coordinate along the 1D domain. In jet diffusion flames, this coordinate represent a radial position; while the temporal evolution may be interpreted as a downstream evolution from the jet inlet if a direct comparison between standalone ODT and experiments are considered. In the above equations, u is the mixture streamwise velocity, which is in the transverse direction of the 1D domain; ρ is the mixture density; Y_α, V_α, $c_{p,\alpha}$, and $\dot{\omega}_\alpha$ are, respectively, the mass fraction, the diffusion velocity, the heat capacity, and the production rate of species denoted with index α. T is the mixture temperature; λ is the mixture heat conductivity; $\bar{c}_p$ is the mixture heat capacity. The thermodynamic pressure, P, is assumed to be spatially uniform and constant. $\dot{\omega}_T$ is the heat release rate term for the temperature equation, which is expressed as follows,

$$\dot{\omega}_T = -\frac{\sum_{\alpha=1}^{N} h_\alpha \dot{\omega}_\alpha}{c_p}, \quad (4)$$

where h_α is the total enthalpy of species denoted with index α. The equation of state,

$$P = \rho \Re T \sum_{\alpha=1}^{N} \frac{Y_\alpha}{W_\alpha},$$

may then be used to compute the mixture density. Here, $\Re$ is the universal gas constant and W_α is the molecular weight for species α. The numerical implementation of the stand-alone ODT solutions is discussed in Ref. [20].

In Ref. [20], the stochastic component of the standalone ODT simulations involved two free parameters. The first parameter, A, is a key parameter in ODT and relates the characteristic time of a selected eddy and the local shear associated with the eddy. The same characteristic time also determines the rate of stirring events. This rate increases proportionally with A; and therefore, given a shear rate field, the rate of stirring may be increased (resp. decreased) by increasing (resp. decreasing) the parameter A without altering the mean shear. Therefore, turbulence conditions may be prescribed by initial conditions with varying shear rates or by changing the value of A.

A second cutoff parameter, β, was implemented to capture the right rate of entrainment in the jet diffusion flame for direct comparison of standalone simulations with experimental data. The parameter was prescribed to prohibit stirring events associated with large eddies, whose characteristic turnover time, $\beta\tau$, is longer than the elapsed time t. Thus stirring events are allowed when $t \geqslant \beta\tau$. The parameter β is chosen to emulate the jet structure near the inlet and the evolving range of scales away from that inlet. As concluded in previous studies [17,18,20], the two ODT parameters, A and β, are responsible for predicting the correct entrainment in the jet diffusion flame. However, in the present simulations, we are primarily interested in reproducing statistics of extinction and reignition in a reduced parameter space. Therefore, the parameter β is set to zero, and stirring events involving the entire range of eddy sizes are allowed at early stages of the temporal jet evolution.

A principal thrust of the present simulation is that variations in either the jet Reynolds number or the parameter A yield essentially the same conditional statistics based on the mixture fraction and temperature; this is established in Section 3.2. Different realizations corresponding to specific initial velocity fields and parameters A are made. These realizations are different by the sequence of random selections of eddy sizes and locations within the 1D domain. The range of run conditions is selected so that both flaming and extinction/reignition solutions are obtained. Favre averages of scalar moment from the different realizations are conditionally averaged upon two parameters: the mixture fraction and temperature. Higher moments can be derived for these scalars as well, in addition to derived scalars, such as heat release or variances of temperature and heat release fluctuations, as discussed below.

2.3. RANS formulation and coupling with ODT

The RANS formulation comprises governing equations in parabolic formulation for the Favre-averaged mean velocity in the predominant flow direction, $\tilde{u}$, mean mixture fraction, $\tilde{Z}$, its variance, $\widetilde{Z''Z''}$, the mean kinetic energy, $\tilde{k}$, its dissipation rate $\tilde{\varepsilon}$, the Reynolds stresses ($\widetilde{u''u''}$, $\widetilde{v''v''}$, and $\widetilde{w''w''}$), and correlations between scalars and velocity terms ($\widetilde{Z''u''}$ and $\widetilde{Z''v''}$). The Favre-averaged radial velocity, $\tilde{v}$, is obtained using the continuity equation. The details of the formulation can be found in Ranganath and Echekki [19], where the formulation was used to model the turbulent H_2–air diffusion flame of Meier and co-workers [21] and Tacke and co-workers [22]. In addition to the above variables, we also solve the transport equations for the Favre mean and the Favre variance of temperature, $\tilde{T}$ and $\widetilde{T''T''}$, which are expressed as follows:

$$\bar{\rho}\tilde{u}\frac{\partial \tilde{T}}{\partial x} + \bar{\rho}\tilde{v}\frac{\partial \tilde{T}}{\partial r} = \frac{1}{r}\frac{\partial}{\partial r}\left(r\bar{\rho} D_t \frac{\partial \tilde{T}}{\partial r} \right) + \widetilde{\dot{\omega}_T}, \quad (5)$$

$$\bar{\rho}\tilde{u}\frac{\partial\widetilde{T''^2}}{\partial x}+\bar{\rho}\tilde{v}\frac{\partial\widetilde{T''^2}}{\partial r}=\frac{1}{r}\frac{\partial}{\partial r}\left(r\bar{\rho}D_t\frac{\partial\widetilde{T''^2}}{\partial r}\right)+2\bar{\rho}D_t\left(\frac{\partial\tilde{T}}{\partial r}\right)^2-\bar{\rho}\tilde{\chi}_T+2\widetilde{T''\dot{\omega}''_T}. \quad (6)$$

The symbol "∼" represents the Favre average. The terms D_t and $\widetilde{\dot{\omega}_T}$ are the turbulent diffusivity of "heat" and heat release terms, respectively. The equation for the mean temperature consists of the convection, the diffusion, and the sink/source terms. A gradient diffusion approximation is implemented for the diffusion term for both $\tilde{T}$ and $\widetilde{T''^2}$. The term $2\bar{\rho}D_t(\partial\tilde{T}/\partial r)^2$ represents a production term for $\widetilde{T''^2}$. The mean temperature dissipation rate term, $\tilde{\chi}_T$, is modeled using an algebraic expression that is similar to the expression used for the mixture-fraction-based scalar dissipation rate,

$$\tilde{\chi}_T=c_\chi\frac{\tilde{\varepsilon}}{\tilde{k}}\widetilde{T''^2},$$

where the time ratio c_χ is set to 2.0 [23]. The last term in the transport equation for $\widetilde{T''^2}$ corresponds to the heat release term contribution.

The mean density, $\bar{\rho}$, and the source terms, $\widetilde{\dot{\omega}_T}$ and $\widetilde{T''\dot{\omega}''_T}$, are the coupling parameters between RANS and ODT. The density and source terms in the 2D table from ODT are functions of instantaneous mixture fraction and temperature. These instantaneous quantities are weighted by the joint PDF of mixture fraction and temperature to obtain the required mean quantities. In the present study, the joint probability density function (PDF) of the mixture fraction and a normalized temperature is expressed as the product of the marginal PDF for Z and the PDF of the normalized temperature conditioned on the Z. The validity of this assumption has been verified by Rullaud [24] for the flames considered in the present study based on the appropriate choice of a progress variable. The β-PDF function is assumed to compute the shape of the PDF of mixture fraction and temperature. This choice of the PDF shape clearly is not justified under all conditions considered, especially during the stages of extinction and reignition. Indeed, Barlow and Frank [10] have shown that during these stages, conditional reactive scalar PDFs exhibit bimodal shapes reflecting conditions of burning and extinction. Therefore, a refined model for these conditional PDFs may be needed to improve the predictions of reactive scalar statistics in moment-based approaches. The PDFs are expressed as

$$P\big(\phi;\tilde{\phi},\widetilde{\phi''^2}\big)=\frac{\phi^{\alpha-1}(1-\phi)^{\beta-1}}{\Gamma(\alpha+\beta)}\Gamma(\alpha)\Gamma(\beta),$$

$$\alpha=\tilde{\phi}\left[\frac{\tilde{\phi}(1-\tilde{\phi})}{\widetilde{\phi''^2}}-1\right]\quad\text{and}$$

$$\beta=(1-\tilde{\phi})\left[\frac{\tilde{\phi}(1-\tilde{\phi})}{\widetilde{\phi''^2}}-1\right]. \quad (7)$$

Here, ϕ corresponds to either the mixture fraction or the temperature. Means and variances for $\widetilde{\dot{\omega}_T}$ and $\widetilde{T''\dot{\omega}''_T}$ are evaluated as follows,

$$\tilde{\psi}=\int_{T_{\min}}^{T_{\max}}\int_0^1\psi(Z,T)P\big(Z;\tilde{Z},\widetilde{Z''^2}\big)\times P\big(T;\tilde{T},\widetilde{T''^2}\big)\,dZ\,dT, \quad (8)$$

where $\widetilde{\psi}$ represents the scalars, $\widetilde{\dot{\omega}_T}$ and $\widetilde{T''\dot{\omega}''_T}$. Note that $\widetilde{T''\dot{\omega}''_T}$ is evaluated from $\widetilde{T\dot{\omega}_T}-\tilde{T}\widetilde{\dot{\omega}_T}$. The scalars ψ inside the integrals in Eq. (8) are evaluated from tabulated ODT statistics. In the above integral, $T_{\min}$ and $T_{\max}$ cover the entire temperature range in the computations and the experiment; they are chosen here as 300 and 2500 K, respectively. The same expression is used for other scalars, except for density, for postprocessing based on the 2D table, $\psi(Z,T)$, and the mixture and temperature PDFs. The mean density, $\bar{\rho}$, is expressed as follows:

$$\bar{\rho}=\left[\int_{T_{\min}}^{T_{\max}}\int_0^1\frac{P(Z;\widetilde{Z},\widetilde{Z''^2})P(T;\widetilde{T},\widetilde{T''^2})}{\rho}\,dT\,dZ\right]^{-1}. \quad (9)$$

To simplify the analysis, the temperature is normalized to range between 0 and 1,

$$T^*=\frac{T-T_{\min}}{T_{\max}-T_{\max}}, \quad (10)$$

such that the limits on the temperature values above also range from 0 to 1. The schematic of the above procedure is shown in Fig. 1. The thick solid lines represent integration within the RANS solver, whereas the thin solid lines represent the one-time generation of the ODT tables. The dashed lines represent postprocessing for obtaining the complete set of solutions. Closure obtained by this procedure depends on the assumption of the shape of the PDF for the reactive scalar.

At this stage of the model formulation, it is useful to discuss briefly some of the attributes of the proposed model compared to other moment-based strategies that have been adopted recently to address the problem of extinction and reignition. Here, we cite more specifically two approaches. In the model by Bradley et al. [25], the PDF of a reaction progress

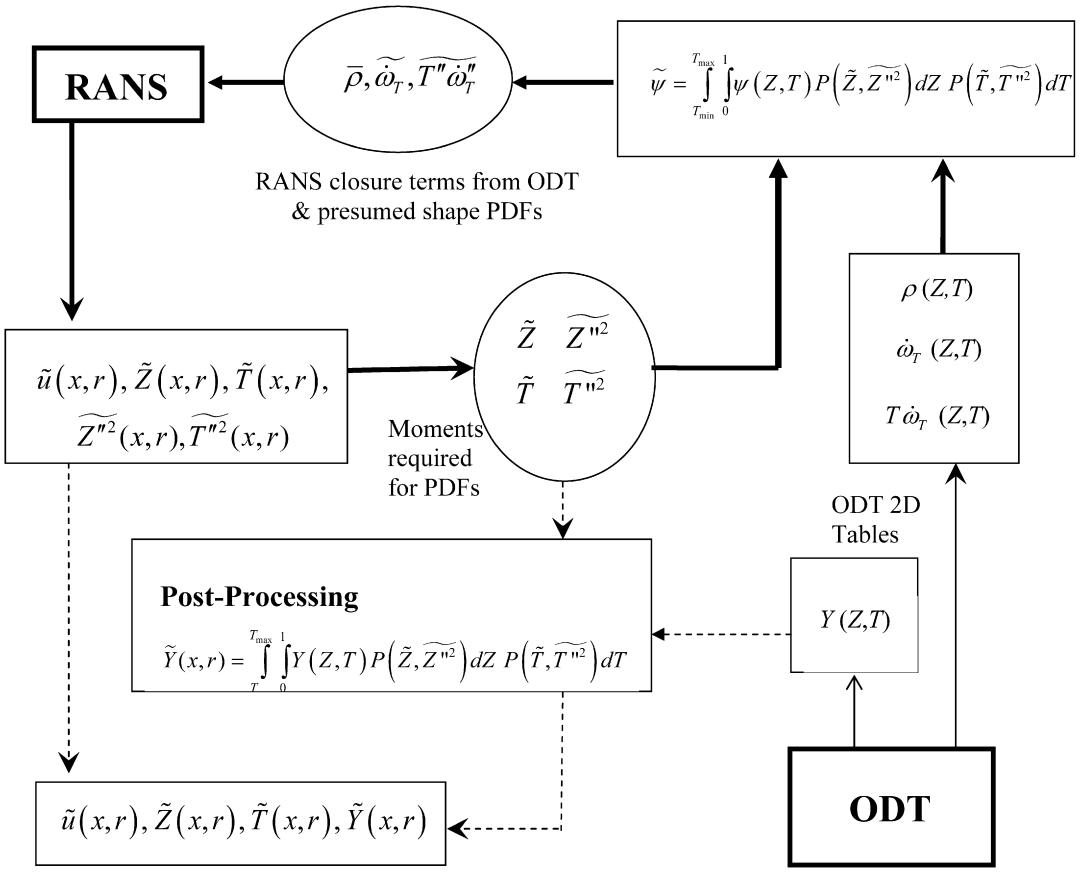

Fig. 1. Schematic of ODT based closure approach adopted for RANS solver.

variable conditioned on the mixture fraction is constructed using a presumed PDF shape and a correction accounting for the extinction using a probability-of-burning function, P_b. P_b represents the probability that the range of straining conditions can sustain flamelet burning. Therefore, it represents a correction to the presumed PDF, which accounts for conditions of extinction. Similarly to the present model formulation for the prediction of scalar statistics, a β-PDF shape is assumed for the conditional PDF for the progress variable. This is clearly a limitation in both the present approach and that of Bradley et al. [25]. Conditional moment equations based on the mixture fraction as the conditioning variable are solved for reactive scalars with source terms constructed using the presumed shape PDFs for the progress variable and the probability of burning function. Both information about the parameterized instantaneous heat release and the probability-of-burning fraction are constructed from flamelet libraries under different conditions of strain rate. The ODT model potentially offers significantly more flexibility than the flamelet approach in generating different burning modes (premixed and nonpremixed), representing the coupling of turbulent transport with the molecular processes of reaction and diffusion and representing different mechanisms of extinction and reignition. As shown later, standalone ODT simulations can reproduce conditions of extinction and reignition and transitions between them within the same simulation. Important transient effects that can affect statistics of scalars associated with slow and fast chemistries are better represented with an unsteady simulation. There is no explicit account for the role of extinction in terms of a probability of burning fraction in the present ODT-based model, although the 2D conditional statistics of reactive scalars does include some extinction and reignition effects, coupled with the response of temperature under different mixture conditions. However, we believe that perhaps a better approach to addressing both conditions of extinction and burning is through an improved model for the presumed PDF shape for reactive scalars. In many respects, P_b represents a factor that accounts for burning mode in the bimodal distribution of the reactive scalars.

In the model by Vervisch et al. [26], the presumed conditional moment (PCM) model is combined with flame-tabulated chemistry (FTC). In FTC, statistics of

reactive scalars are conditioned as functions of the mixture fraction and a reaction progress variable as implemented here. However, the sources of the tabulation are fundamentally different. In [26], the FTC tables are constructed through a weighted contribution of nonpremixed and premixed flame contributions. Therefore, FTC may be viewed as a correction to the reactive scalars level under purely nonpremixed conditions and a way to account for the presence of extinction through laminar premixed flames tables. Again, there is no explicit account for the mechanism of reignition here. The FTC tabulation adds an additional level of models to evaluate the contribution to the scalar statistics of the different modes of combustion (premixed vs nonpremixed) and to account for the prediction of species associated with slow chemistry (e.g., NO). Similarly to the strategy adopted for the ODT-based approach, the joint PDF of the mixture fraction and the progress variable are evaluated as the product of the mixture fraction marginal PDF and the progress variable conditional PDF using β-function shapes for the two PDFs and without correction for a probability-of-burning function. Comparisons of reactive scalars' predictions based on the PCM-FTC model yield reasonable predictions for flame D [24,26] and the right trends for flame F [24]. Overall, we believe that the present model offers a number of important advantages in comparison with flamelet models. There is no inherent assumption about the burning mode; therefore, joint statistics of the mixture fraction and the progress variable may be constructed within the same simulation. Additional conditioning variables may be added if needed to predict other pertinent statistics if needed within the context of a single simulation. Moreover, molecular chemistry and transport are coupled with turbulent transport; and finally, an unsteady model can account for important transient responses to address at the same time the prediction of species associated with fast and slow chemistries.

3. Results and discussion

In this section, we present and discuss results of the ODT-based closure approach within the context of a moment approach to turbulent combustion. Here, spatial profiles in terms of axial and radial statistics are presented for the streamwise velocity, the mixture fraction, and reactive scalars. While it is customary to use conditional statistics for comparison with experiment [10] based on a single conditioning variable, such as the mixture fraction, these singly conditioned statistics are replaced here by doubly conditioned statistics and spatial statistics.

3.1. Run conditions for RANS simulations

The model is implemented to simulate the structure of a piloted methane–air jet diffusion flame measured at Sandia National Laboratories [10]. The experiment was carried out for a range of flow conditions. In the present study, only three conditions are considered, which correspond to flames D, E, and F and display increasing degrees of extinction as the Reynolds number is increased. The fuel composition is 25% methane and 75% air exiting from the central nozzle. The inner diameter of the nozzle is $d = 7.2$ mm. The bulk velocities of the jet are 49.6, 74.4, and 99.2 m/s, which correspond to Reynolds numbers based on the jet diameter of 22,400, 33,600, and 44,800 for flames D, E, and F, respectively. The pressure is measured at 0.993 atm. The flame is stabilized by a pilot premixed flame consisting of a lean mixture (equivalence ratio $\phi = 0.77$) of C_2H_2, H_2, air, CO_2, and N_2 with the same enthalpy and equilibrium composition as methane–air at the same equivalence ratio. The flow parameters for flames D, E, and F are given in Table 1. The initial pilot composition and temperature are given in Table 2. The bulk velocity of the pilot flame is 11.4, 17.1, and 22.8 m/s for flames D, E, and F, respectively. The annulus of the pilot flame has an inner diameter of 7.7 mm and an outer diameter of 18.2 mm. The coflow air flows between the burner outer wall (18.9 mm diameter) and the square

Table 1
Flow parameters at the inlet based on the experimental conditions

Flame	Re_d	U_{fuel} (m/s)	U_{pilot} (m/s)	U_{coflow} (m/s)
D	22,400	49.6	11.4	0.9
E	33,600	74.4	17.1	0.9
F	44,800	99.2	22.5	0.9

Note. The velocities represent bulk properties at the fuel jet, the pilot, and the coflow.

Table 2
Pilot temperature and composition (mass fractions) at the jet inlet

T (K)	1880
ρ (kg/m^3)	0.180
Y_{N_2}	0.7342
Y_{O_2}	5.4×10^{-2}
Y_O	7.47×10^{-4}
Y_{H_2}	1.29×10^{-4}
Y_H	4.8×10^{-6}
Y_{H_2O}	9.42×10^{-2}
Y_{CO}	4.07×10^{-3}
Y_{CO_2}	0.1098
Y_{OH}	2.8×10^{-3}

wind tunnel inlet (30 cm each side). The coflow bulk velocity is 0.9 m/s. The initial fuel jet profiles are obtained from channel flow simulations using ODT that yield fully developed velocity profiles at the jet inlet. The ratio of the fuel and air densities is 0.88.

The experimental database includes simultaneous point measurements of temperature using Rayleigh scattering, concentrations of CH_4, N_2, O_2, CO_2, H_2O, and H_2 using Raman scattering, and OH, NO, and CO concentrations using laser-induced fluorescence. Velocity measurements at the Technical University at Darmstadt were made using LDV for flame D [27].

As outlined earlier, standalone ODT simulations are implemented to generate a 2D conditional statistics table for the postprocessing reactive scalars (primarily reactive species concentrations) and closure terms in the RANS governing equations (mean density and source terms in the mean and variance of temperature). Top hat profiles for the species concentrations and the velocities are prescribed at the inlet (i.e., initial conditions). The chemistry is based on the reduced 12-step mechanism of Sung et al. [28], consisting of 16 species, H_2, H, O_2, OH, H_2O, HO_2, H_2O_2, CH_4, CO, CO_2, CH_2O, C_2H_2, C_2H_4, C_2H_6, and N_2, respectively.

In contrast with the experimental conditions, different mixing conditions are imposed by varying the ODT parameter A and the jet Reynolds number. In total, 14 different conditions are run, each involving approximately 300 realizations. However, only a small fraction of these realizations is actually needed to capture the 2D conditional statistics. Generally, around 100 realizations are sufficient to obtain adequate statistics for densities and other reactive scalars conditioned upon the mixture fraction and temperature, whereas the source term for temperature and its variance require close to 200 realizations to obtain reasonably smooth statistics. The different conditions correspond to two values of $A = 0.344$ (the original value) and 0.0172 (5% of the original value) and seven jet Reynolds number conditions ranging from 16,800 to 50,400 at equal increments of 5600. The different realizations for the same condition correspond to the same inlet conditions but different histories of the stochastic implementation of stirring events.

The 2D reduced table is based on double-conditioning scalar moments with respect to mixture fraction and temperature. ODT simulation results are output at different time increments of the ODT solution evolution and accumulated over realizations, time, and spatial grids. The resulting database is the source for the statistics. Furthermore, appropriate boundary conditions are provided, and the interpolation scheme by Akima [29] is employed to obtain a 2D table on a Cartesian grid of the mixture fraction and temperature. These conditions correspond to pure mixing conditions at $Z = 0$ and 1.

Three different RANS simulations are carried out that correspond to inlet conditions for flames D, E, and F in the experiment. All initial scalar profiles are prescribed with a Heaviside function for temperature and mixture composition, as given in Table 2. Turbulence momentum terms are based on LDV measurements [27], which include 2D components of the Reynolds stress, $\widetilde{u''u''}$, $\widetilde{v''v''}$ and $\widetilde{u''v''}$. The components $\widetilde{w''w''}$ and $\widetilde{u''w''}$ are set as equal to $\widetilde{v''v''}$ and $\widetilde{u''v''}$, respectively, and the turbulent kinetic energy is prescribed as follows:

$$k = \frac{1}{2}\left(\widetilde{u''v''} + \widetilde{v''v''} + \widetilde{w''w''}\right).$$

The turbulence dissipation rate, ε, is prescribed based on a mixing length formulation. The scalar transport terms, $\widetilde{u''Z''}$, $\widetilde{v''Z''}$, and $\widetilde{w''Z''}$ are prescribed as fractions (10%) of $\widetilde{u''u''}$, $\widetilde{u''v''}$, and $\widetilde{u''w''}$, respectively. Symmetric boundary conditions are enforced at the jet centerline and free stream boundary conditions are prescribed at the outer boundary of the solution. The mean density, $\bar{\rho}$, is prescribed directly from the 2D table and the assumed PDF shapes.

3.2. Validation of double conditioning

In this section, first the feasibility of the double conditioning used to provide closure for RANS is addressed. Next, the doubly conditioned statistics from ODT are validated against experiments. This feasibility of double conditioning is achieved by comparing the experimental data for the three flames, Sandia flames D, E, and F, from the series of turbulent CH_4–air jet diffusion flames of Barlow and Frank [10] as follows. The experimental data from these flames are doubly conditioned upon mixture fraction and temperature.

Fig. 2 shows the contour profiles of doubly conditioned density for the three flames D, E, and F, based on experimental data. The figure show no discernable difference between the three flames where common data are found; the only distinction between the different flames stems from differences in the range of conditioning variables spanned by these flames, with flames at higher Reynolds numbers exhibiting broader ranges. Thus, from the figure, we see that the area spanned by flame F in the phase space is greater than that for flame E, and accordingly greater than that for flame D. Therefore, a 2D conditioning table for the density based on flame F can be used for both flames E and D.

Next, we investigate if other reactive scalars, namely species mass fractions, also exhibit the trend

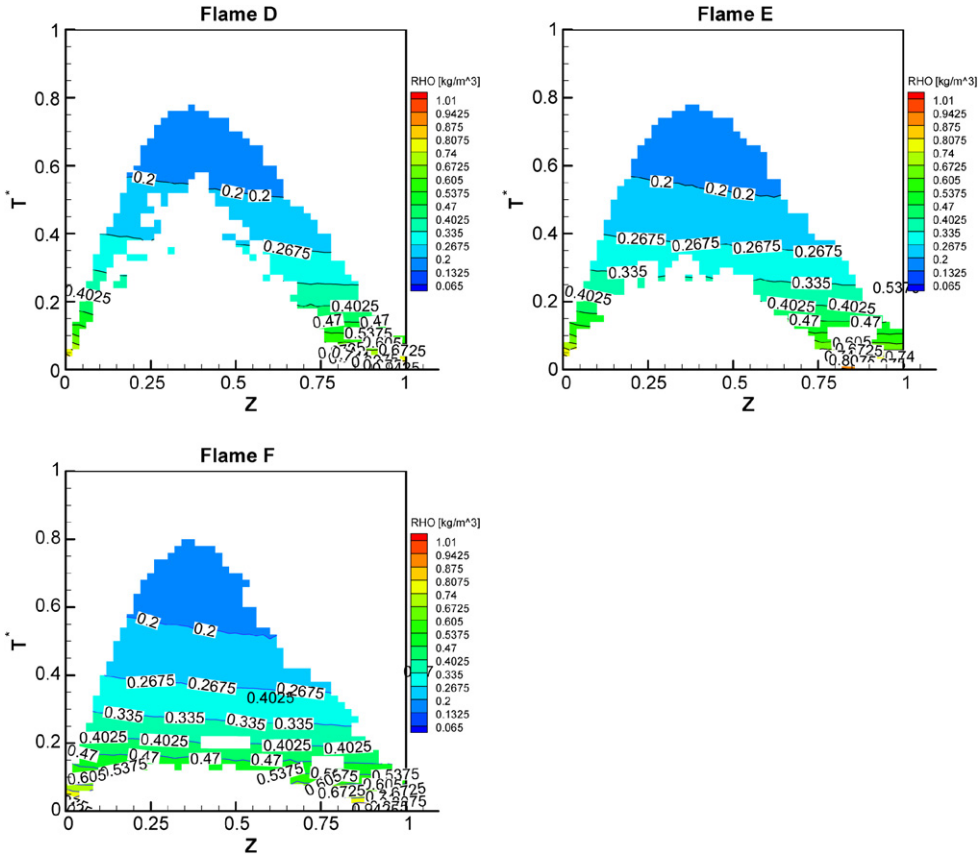

Fig. 2. Comparison of 2D density statistics for flames D, E, and F from experiments.

observed for the density. Here, to be able to make direct comparisons between the flames, we consider cuts of the 2D conditional contours along the stoichiometric mixture fraction. Fig. 3 shows the 1D profiles of density, reactive scalars, H_2O, H_2, and CO, as a function of normalized temperature corresponding to the stoichiometric mixture fraction ($Z = 0.35$) for the three flames D, E, and F, respectively. These profiles are extracted from the 2D conditional means. The figure clearly shows agreement between the different flames' statistics whenever the data ranges in the conditioning variable overlap. Again, and as seen in Fig. 2, the principal difference between the various flames is the range spanned by the temperatures; at higher jet Reynolds numbers the increased rates of extinction result in lower temperature conditions. Similar trends (not shown here) are observed for mixture fraction equal to 0.5, which corresponds to the location of peak intermediate mass fractions in the phase space. Thus, from the above discussion, it can be concluded that one single table, constructed by doubly conditioning on mixture fraction and temperature, is sufficient to represent the process of extinction and reignition in the piloted methane–air flames. These tables may be constructed based on the higher jet Reynolds number conditions.

Next, we evaluate whether the same trends are reproduced by the stand-alone ODT simulations. No distinction between the different jet Reynolds number conditions is made here, because we did not seek a one-to-one correspondence between the run conditions and the experimental data. Instead, all ODT standalone runs are used to construct a single 2D conditioning table. As mentioned in the previous section, ODT simulations are obtained by varying the jet Reynolds number and the ODT parameter, A, with each ODT simulation exhibiting varied degrees of turbulence–chemistry interaction. Statistics are collected over 200 realizations for each ODT simulation, and parameterized upon mixture fraction and temperature, so that all flame solutions are uniquely represented. In Fig. 4, the doubly conditioned ODT statistics are compared to those obtained from combining the data from the three experimental flames, D, E, and F. The quantities compared are the doubly conditioned densities and CO mass fractions corresponding to all variations of the ODT simulation approach. We see that, overall, there is good agreement

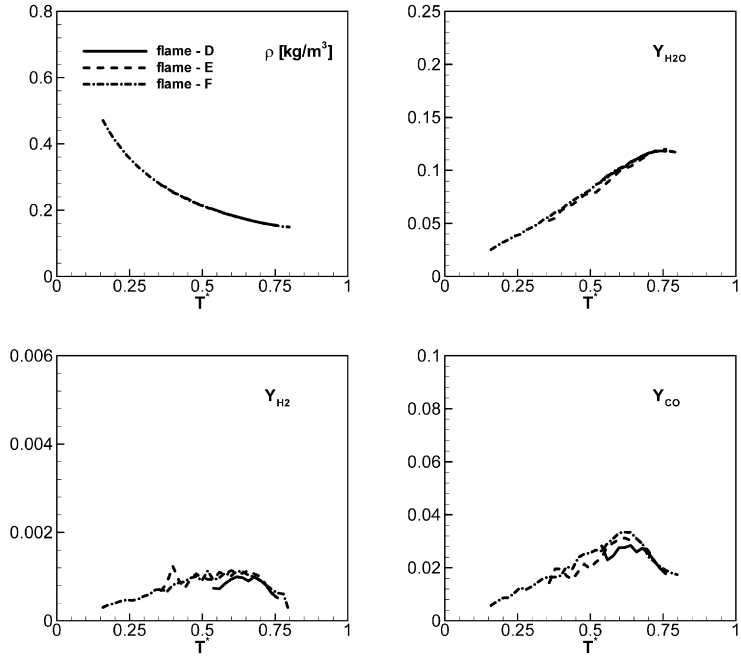

Fig. 3. Comparison of doubly conditioned density and reactive scalars at stoichiometry as a function of temperature for flames D, E, and F from experiments.

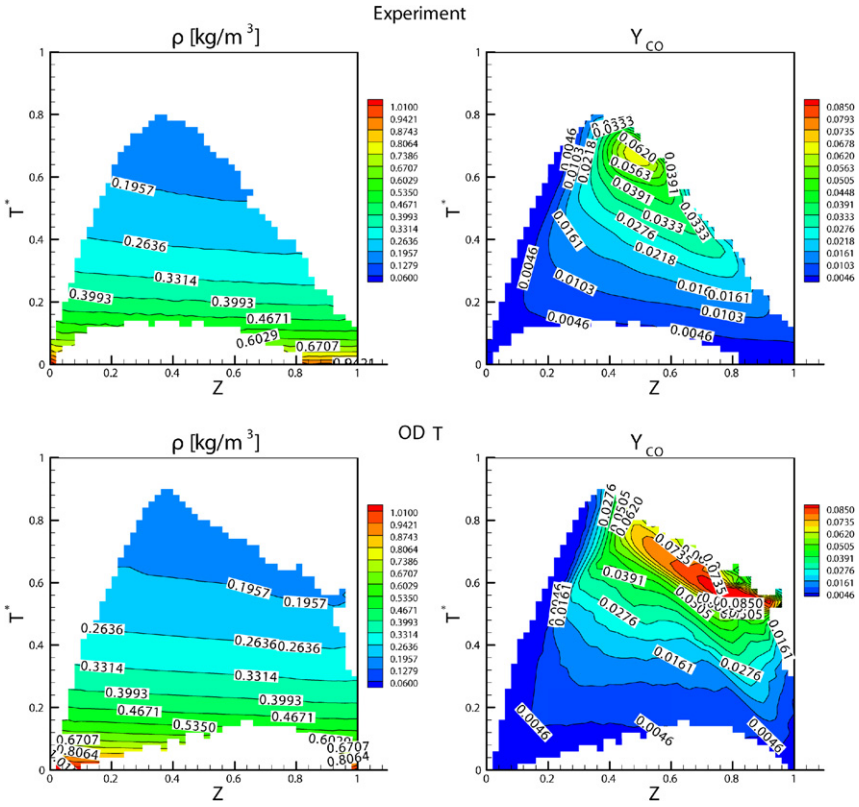

Fig. 4. Comparison of doubly conditioned statistics for density and CO mass fractions from ODT and experiments.

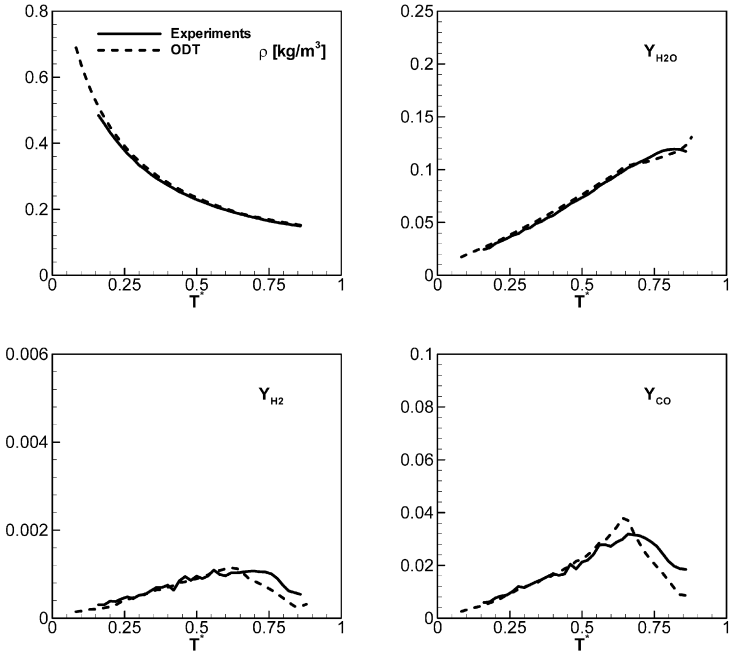

Fig. 5. Comparison of doubly conditioned statistics for density and reactive scalars at stoichiometry as a function of temperature from ODT and experiments.

between the results from ODT and experiments. Similarly to experiments, ODT is able to distinguish between the burning solutions corresponding to higher temperatures and the extinguished ones corresponding to lower temperatures. However, under rich conditions, ODT predicts chemistry as seen in the contour plot of CO mass fractions. Although not shown here, no discernable distinction between scalar statistics is found for the same parameter pairs, Z and T. Therefore, a consolidated table is obtained. The independence of the scalar statistics on the choice of varying the jet Reynolds number or the parameter A is a favorable outcome of the simulation: a simplified flow configuration can yield still meaningful statistics for the problem of extinction and reignition in spatially developing jet diffusion flames.

In Fig. 5, the doubly conditioned ODT statistics are compared to those obtained from experiments corresponding to the stoichiometric mixture fraction. There is excellent agreement between the simulations and experiments for densities and CO mass fractions. It is further observed that ODT provides data corresponding to lower temperature, which only represent a mixing solution and do not influence the closure provided to the RANS solver. Similar observations (not shown here) are obtained at various other mixture fractions and for other species. Although ODT predicts chemistry corresponding to the rich conditions, the agreement between the simulations and experiments is excellent where data from experiments are available. The earlier conversion of the primary fuel, CH_4, to intermediates, CO and H_2, in the case of ODT, can be attributed as one of the reasons for ODT showing chemistry in the rich regions. Also, the mapping events in ODT result in associating the hot products of combustion with the cold unburnt premixed fuel mixture, resulting in a burning solution.

3.3. Axial profiles for flames D, E, and F

As discussed earlier, spatial profiles of scalar statistics are influenced by the different model components associated with moment methods. A reasonably unified reduced-space description is found for the different flames in terms of mixture fraction and temperature. Therefore, differences between RANS–ODT computations and experiment may arise from the remaining two model components, which are associated with the transport equation for the conditioning variables and their presumed PDF shapes.

Fig. 6 compares the axial profiles of mean and RMS (root mean square) of streamwise component of velocity, mixture fraction and temperature, and mean density for major and intermediate species mass fractions with experiments for flames D (Fig. 6a), E (Fig. 6b), and F (Fig. 6c). The figures show that the evolution of the mean and RMS values of the mixture fraction along the axis is reasonably predicted for flames D, E, and F. The predicted flame heights, corresponding to the position of the mean mixture frac-

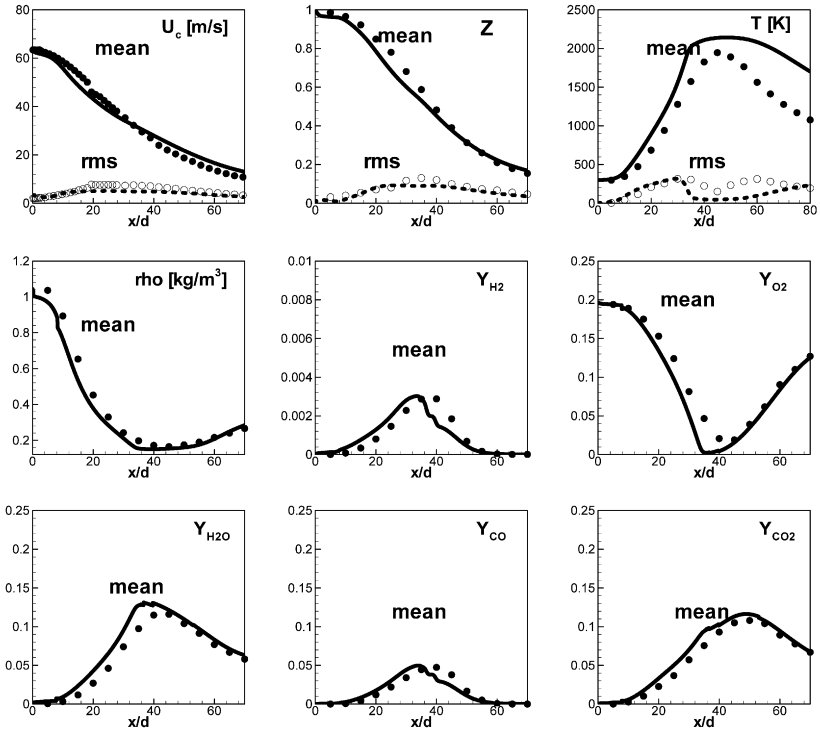

(a)

Fig. 6. Comparison of axial profiles of mean and RMS for velocities, mixture fraction and temperature, mean density and reactive scalars from simulation and experiments for flames (a) D, (b) E, and (c) F. The symbols represent experiments and lines simulations.

tion of 0.35, are in very good agreement with the experimental heights (within one diameter for the worst case, flame E). For the streamwise velocity, the RMS values are well predicted, while the mean streamwise velocities indicate faster decay for flame F.

From the figure, we see that the temperature is in good agreement with the experiments for the first 20 jet diameters for flames D and E. For flame F, the computed profiles overpredict the experimental profiles starting as early as $x/d = 10$. Nonetheless, from this position and beyond, the correct shapes and locations of the peaks are predicted by the simulations. Since the temperature is a transported variable in the present RANS formulation, the principal contribution to the discrepancy between computed and measured mean temperatures may be attributed to the balance between the turbulent diffusion term in the governing equation for temperature and the source term. This latter term results from combining the looked-up doubly conditioned means from the 2D table and the presumed PDFs of both the mixture fraction and the temperature. Therefore, a larger source of uncertainty is associated with the evaluation of the transport equation for the temperature. Correspondingly, the densities are well predicted up to the flame height, and beyond it are in excellent agreement with the experiments for flames D and E. For flame F, there are discernable discrepancies between the measured and computed densities. These differences may largely explain the differences between the axial profiles of the streamwise velocities, since the density is the principal parameter that couples all the transport equations in RANS.

An alternative presentation of the axial profiles is shown in Fig. 7, which shows the axial profiles presented in Fig. 6 as a function of the mean centerline mixture fraction. By the choice of this alternative coordinate, we attempt to attenuate contributions from the RANS formulation, its model constants, and the initial profiles adopted for the various transported quantities. Fig. 7 shows that the agreement between experiment and computed is improved when the profiles are superposed in terms of the centerline mixture fraction for flames D and E and for temperature, density, and species mass fraction profiles shown. For flame F, important differences between the computed and measured profiles are still present near the inlet and up to the flame height (the centerline mixture fraction value of 0.35). Nonetheless, peak and minimum values and the corresponding position for

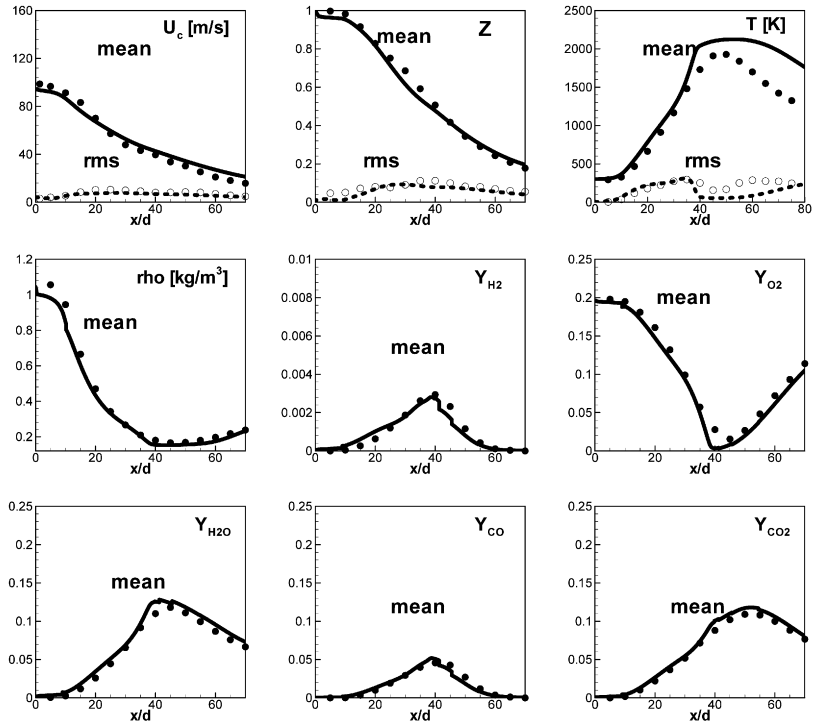

(b)

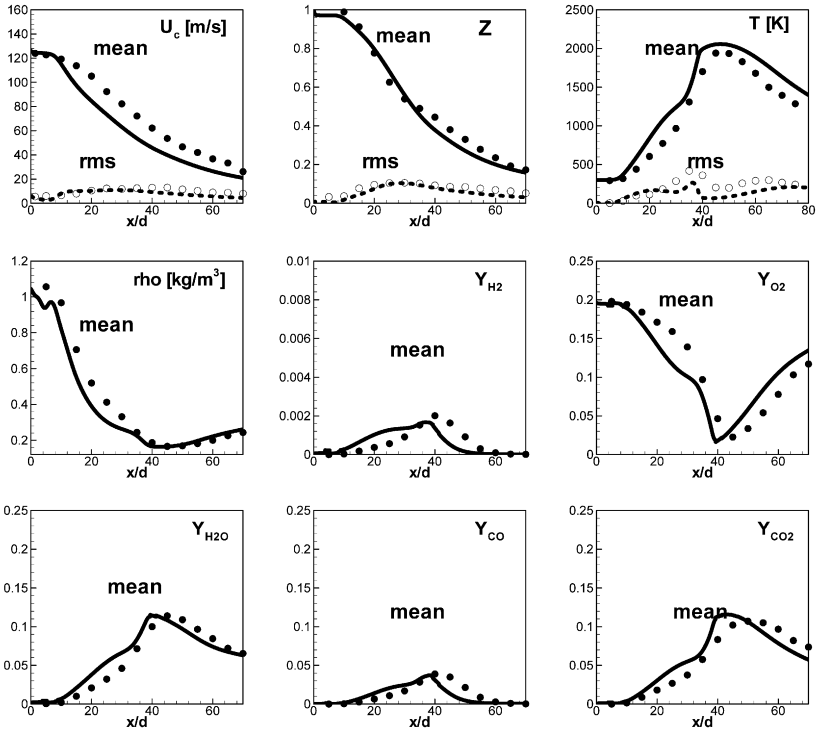

(c)

Fig. 6. (*continued*)

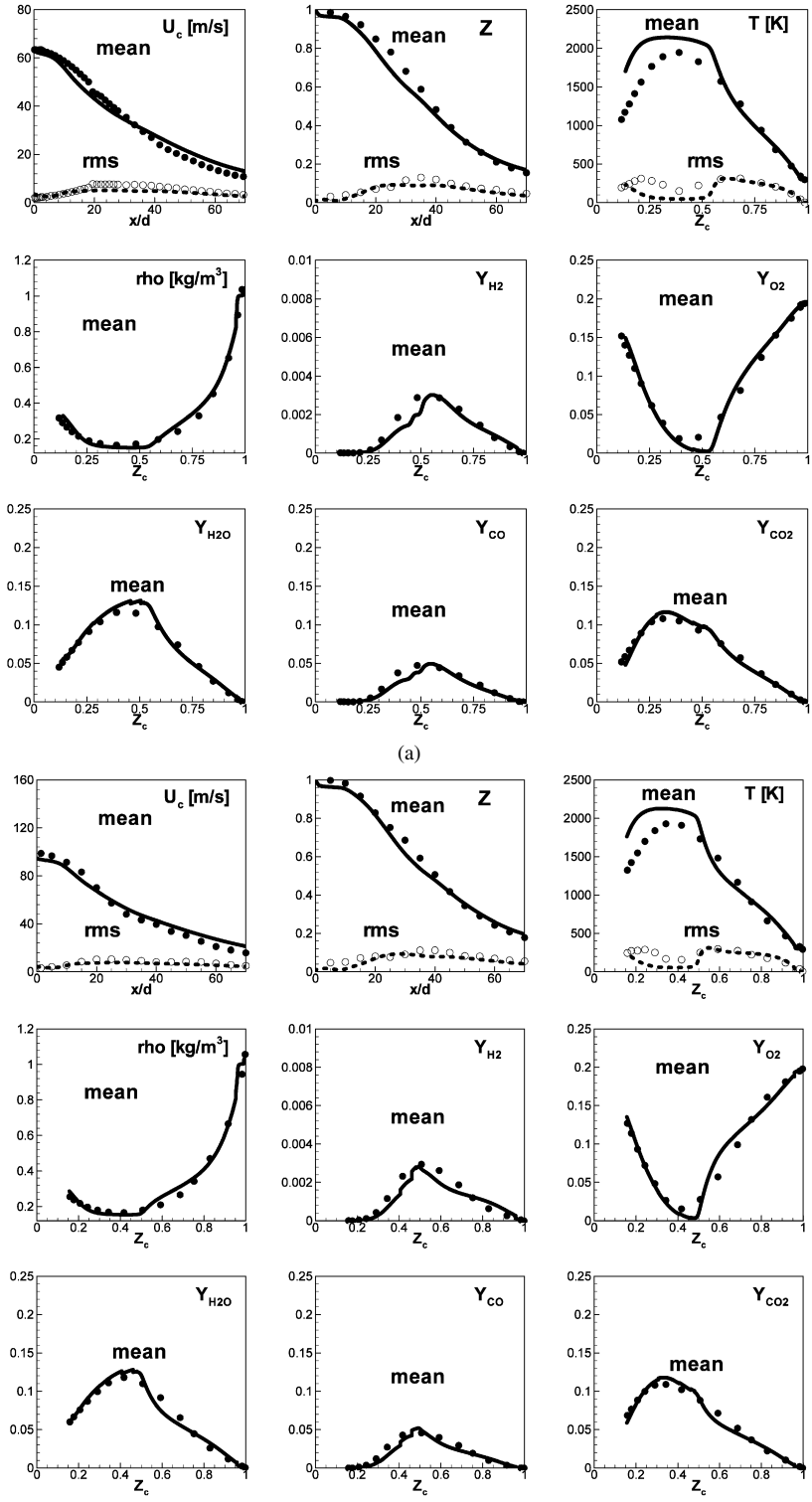

Fig. 7. Comparison of axial profiles of mean and RMS for velocities, mixture fraction and temperature, mean density and reactive scalars from simulation and experiments for flames D (a), (b) E, and (c) F, in phase space. The symbols represent experiments and lines simulations.

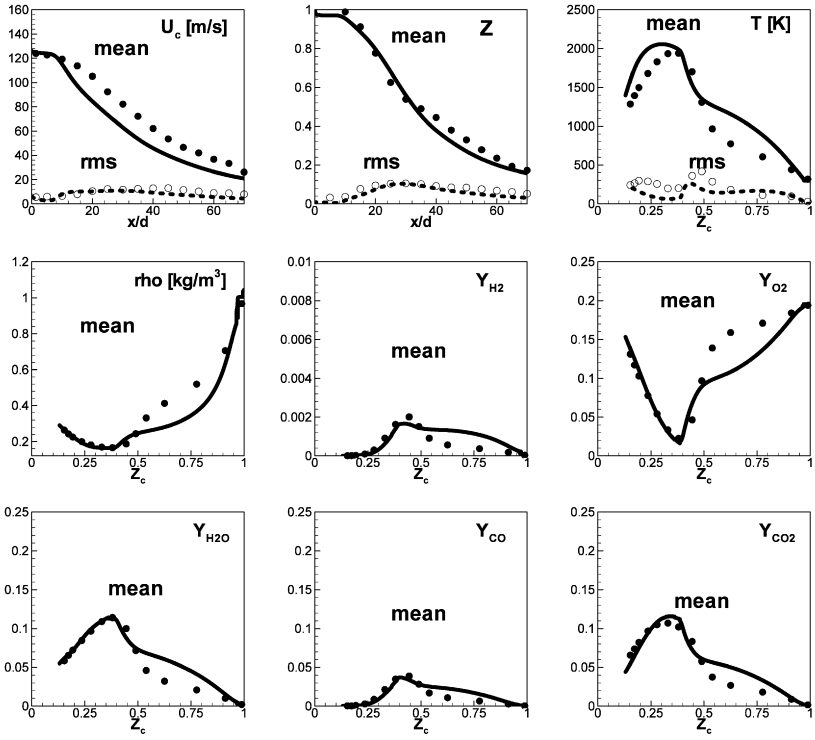

(c)

Fig. 7. (*continued*)

the density and species mass fractions are well predicted. Moreover, the agreement between measured and computed statistics for the density and species mass fractions is excellent past the flame height for all flames. This agreement reflects the fact that a single unimodal PDF is recovered again once the ignition process is completed. This agreement must be contrasted with that of the temperature at downstream distances beyond the flame height. Again, the temperature profiles are generated by the integration of the RANS equations; and therefore, it is subject to both RANS model contributions and the 2D table contribution represented in the heat release term. Another important observation at these downstream distances is that the predictions of species mass fraction profiles are more likely to be governed by a single parameter, the mixture fraction, consistent with what has been adopted in the original formulation of the flamelet and CMC approaches. In contrast, the 2D conditioning table is needed to adequately predict the processes of extinction and reignition in flames D, E, and F.

Based on the above observations, the rate of entrainment to the centerline is reasonably predicted, as shown by the axial profiles of the mean mixture fraction and its variance. The model prediction of $\bar{\rho}$ from the ODT table and the assumed shape PDF is excellent for flames D and E and yields discernable discrepancies in flame F. The mean density couples various variables in the RANS solution vector; therefore, its prediction influences the solution of all variables in that solution vector. The discrepancy between predicted and measured statistics in flame F may be attributed to corresponding higher mean temperatures, as shown in Fig. 6c, and despite the fact that the temperature RMS predictions are reasonable in the first 20 diameters. Temperature profiles are governed by the balance of the source term and the scalar flux term $\widetilde{u''T''}$, which is treated here with a gradient diffusion model. Our computations show that the difference between the two quantities, at certain stages of the solution, can have a much lower magnitude than the flux or source terms. Other factors involved in the solution for $\widetilde{T}$ and its variance include the assumed temperature PDF shape.

3.4. Radial profiles for flames D, E, and F

Figs. 8 to 11 compare the radial profiles obtained from simulations against experiments at $x/d = 7.5$, 15, 30, and 45, respectively. The quantities compared are the mean and RMS of mixture fraction and temperature and the means of reactants O_2 and CH_4, products CO_2 and H_2O, and intermediates CO and H_2. The effects of inlet conditions of turbulence and

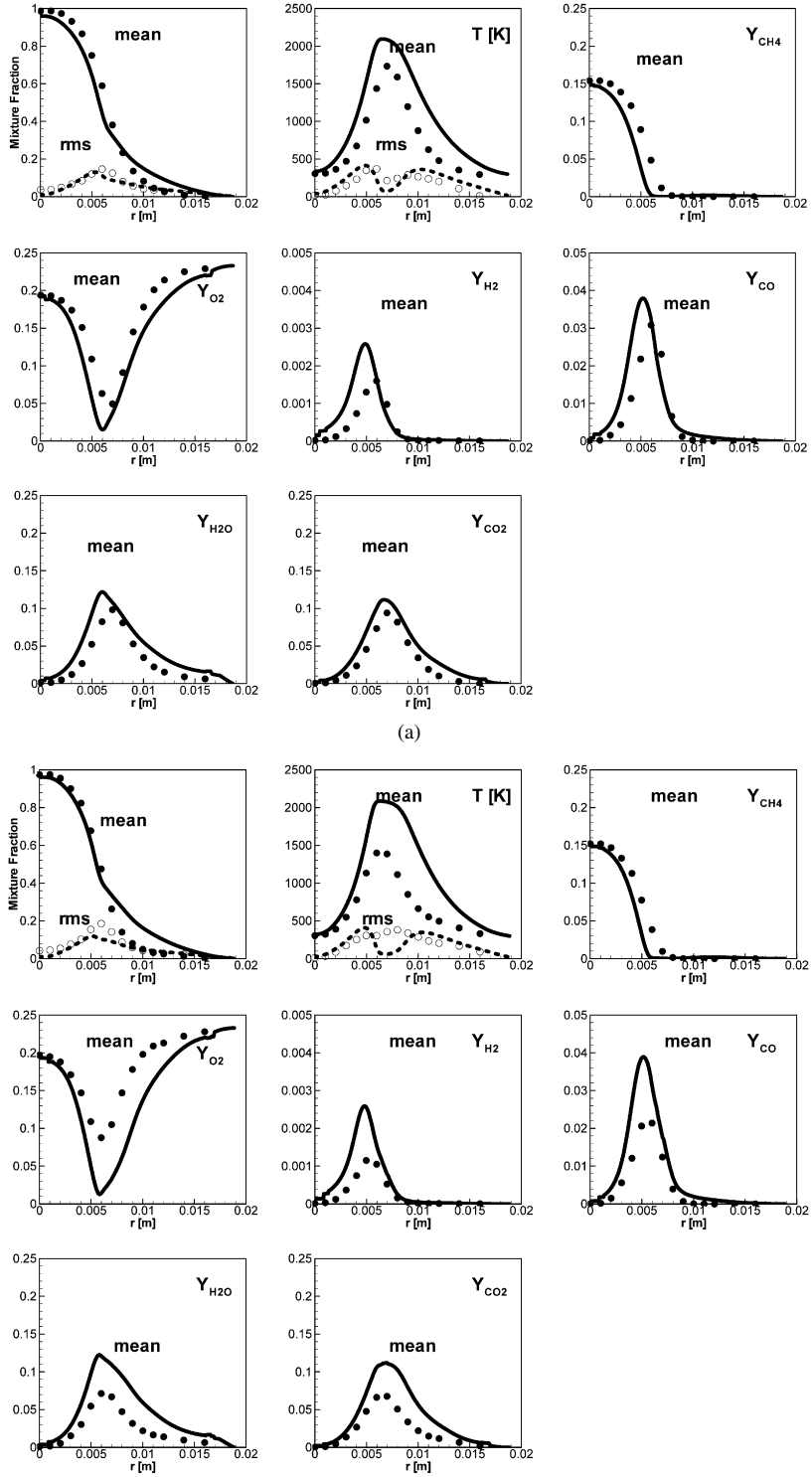

Fig. 8. Comparison of radial profiles of mixture fraction and reactive scalars from simulations and experiments for flames (a) D, (b) E, and (c) F, at 7.5 jet diameters. The symbols represent experiments and lines simulations.

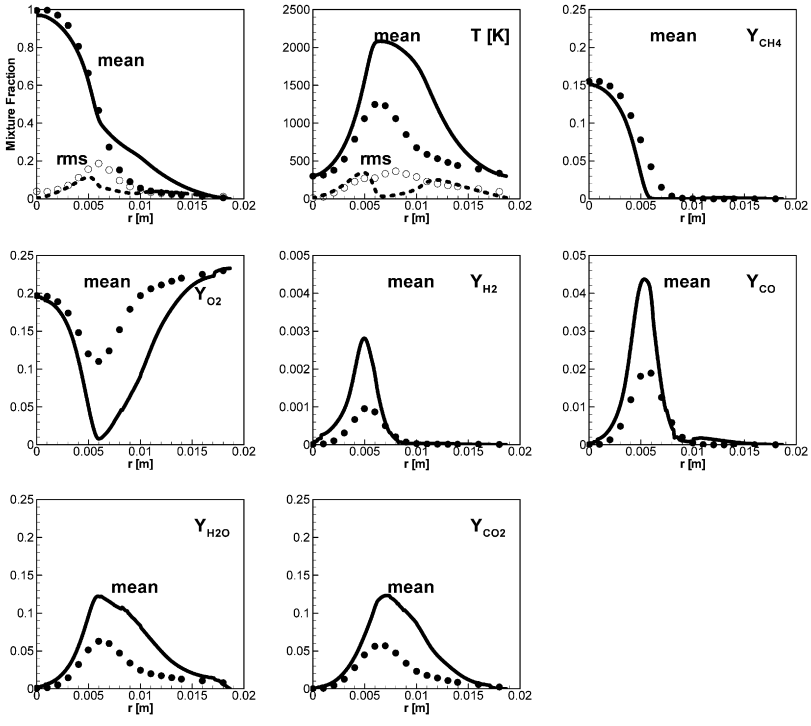

(c)

Fig. 8. (*continued*)

scalar profiles are seen at $x/d = 7.5$. As shown in Fig. 8, at $x/d = 7.5$, we see that the computed values decay at a higher rate in the fuel-rich region and are overpredicted in the coflow. Nonetheless, the mean profile shapes for temperature are well predicted by the simulation for flame D; however, the maximum temperature is not suppressed well enough compared to the experiments. Correspondingly, the flame D temperature RMS is underpredicted at the peak location, indicating less mixing in the computations than in the experiments. Although not shown here, simulations with different initializations for Reynolds stresses, turbulent kinetic energy, and its dissipation rate may be fine-tuned to improve the prediction of scalar statistics in the near field. However, to retain consistency with the experiments, the turbulence and scalars for RANS simulations are not altered and initialized from the experiments.

Important differences between peak values of temperature for flames E and F are found at $x/d = 7.5$. In contrast with experiment for flame D, the corresponding peaks for temperature are a few hundred degrees lower for flame E, and a more dramatic difference is found for flame F. Extinction is already present in the experimental results; while the computational data do not exhibit any large differences between the different flames. The peak value of the experimental RMS also indicates the presence of both ignited and extinguished flamelets, while the computed profiles indicate a local minimum at high temperature, consistent with the standard burning solution. Therefore, the RANS-ODT solution is characterized by a delay in the onset of extinction. Again, fine-tuning the turbulence conditions helped in establishing the experimental trends for flames E and F.

The qualitative difference is already present in the reactive scalar statistics for O_2, CH_4, CO_2, and H_2O. The ODT predictions for flame D are reasonable, but substantially more extinction is found in the experiment at $x/d = 7.5$. For these scalars, this extinction is exhibited by higher product means in the computed profiles. Intermediate species means for H_2 and CO are overpredicted by the computations, and these overpredictions are more pronounced at higher jet Reynolds numbers. Similar observations are found in the simulations by Pitsch and Steiner [30] for flame D, which they attribute to the already premixed nature of the fuel. However, the recent simulations by Cao and Pope [31] suggest that the ARM mechanism yields predictions similar to those of the detailed mechanism for scalar statistics. In the present case, we believe that the discrepancy is due to deficiency in the prediction of the temperature variance, which results in higher temperature and combustion in the fuel-rich region. As mentioned above, adjusting the initial profiles for the dissipation rate of turbulent kinetic energy

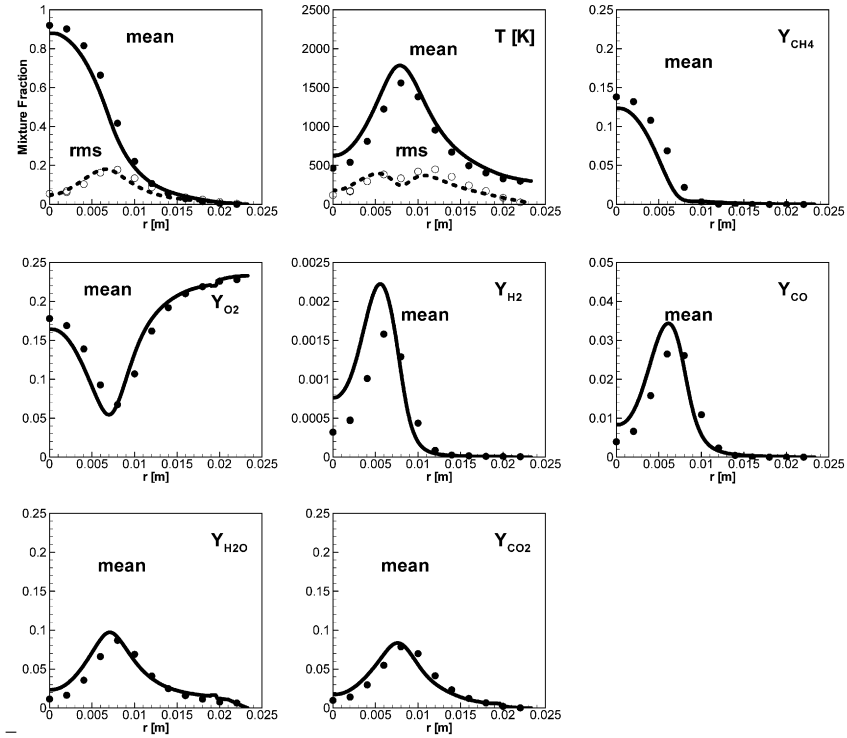

(a)

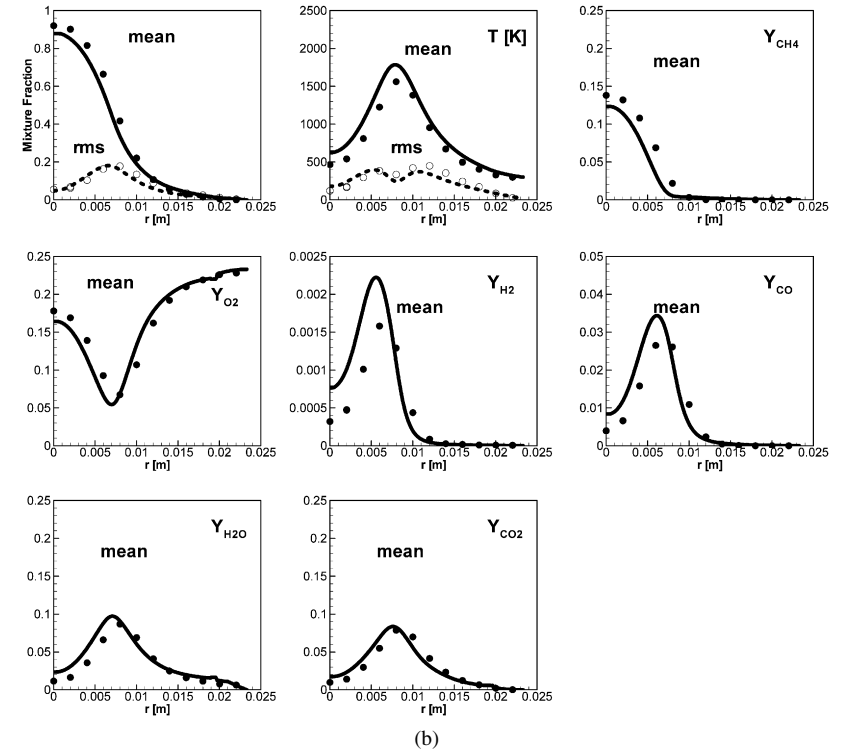

(b)

Fig. 9. Comparison of radial profiles of mixture fraction and reactive scalars from simulations and experiments for flames (a) D, (b) E, and (c) F, at 15 jet diameters. The symbols represent experiments and lines simulations.

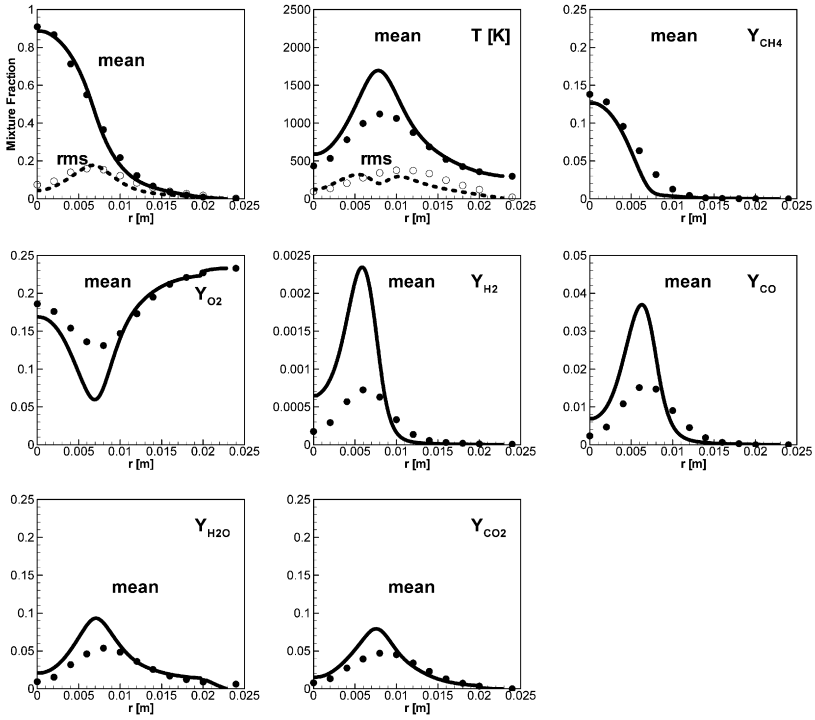

(c)

Fig. 9. (*continued*)

has improved the predictions for temperature, resulting in reasonable agreement for the intermediates in the near field.

Fig. 9 compares the same set of quantities at $x/d = 15$. As observed in the axial profiles, the mixture fraction and temperature profiles spread at a faster rate toward the centerline as compared to the experiment. By this downstream distance, the effects of the initial profiles are less significant, resulting in good predictions of mean mixture fraction and temperature. Moreover, their RMS is also in good agreement with experimental data for all flames considered. Reactive scalar profiles at $x/d = 15$ still show a consistent delay in the onset of extinction in the flames indicated in the computed statistics by slightly higher peak temperatures, higher intermediate mass fraction means and higher products mass fractions. Again, the discrepancy between computed and measured statistics is higher at higher Reynolds numbers (flames E and F). The location of peak values for reactive scalar means is reasonably well predicted. ODT also predicts the qualitative trends of the experimental data corresponding to increased rates of extinction at higher Reynolds numbers; peak temperatures are higher for the lower jet Reynolds number flames.

Fig. 10 compares the radial profiles from the simulations with the experiments at $x/d = 30$. At this downstream distance, the reignition process has already started in the flames, but it is not complete. However, the simulations show complete recovery to a burning solution as compared to the experiments. As observed at the previous axial location, the mixture fraction from the simulations decays at a higher rate compared to experiments, resulting in lower predictions of reactants, O_2 and CH_4, and higher predictions of products, H_2O and CO_2, and intermediates, CO and H_2, at the centerline. The discrepancy between computed and measured statistics at the axis (i.e., radial location of 0) is more pronounced for flames D and F, and less significant for flame E. Moreover, the positions of the peaks of means of temperature and intermediate species are shifted more toward the axis in the computed statistics. The corresponding RMS values are reasonable for flames D and E and lower for the computed values in flame F, even though the RMS of the mixture fraction is well predicted in all flames at $x/d = 30$. The low RMS values for temperature and their corresponding higher means are the principal mechanisms for the trends observed in the mass fractions of reactants, products, and intermediates. As stated earlier, the Favre mean and RMS of the temperature are computed using transport equations, and potential refinements in these closure models for these equations may results in improvements in reactive scalars statistics that are subject to the predictions of the moments of the temperature.

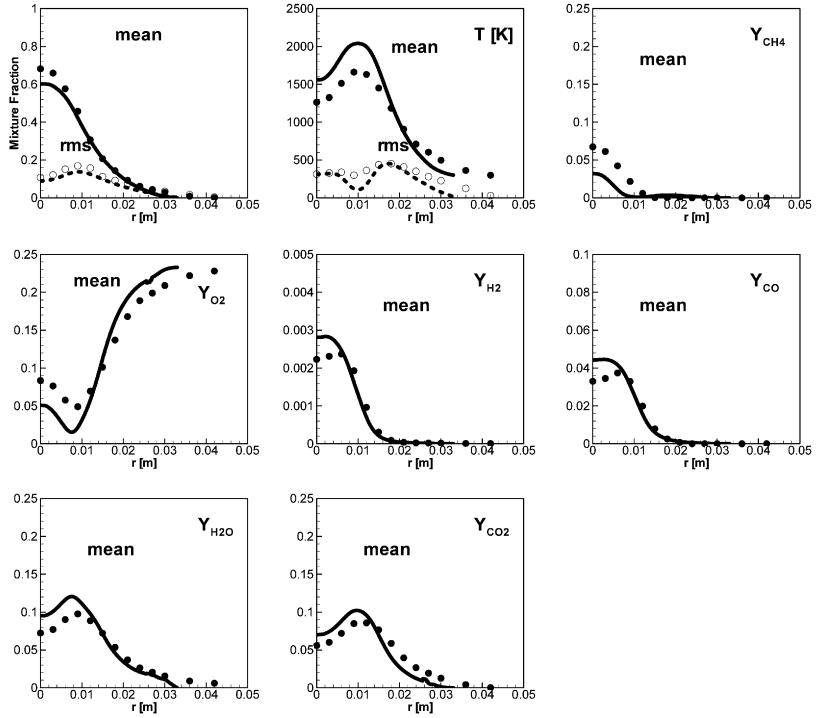

(a)

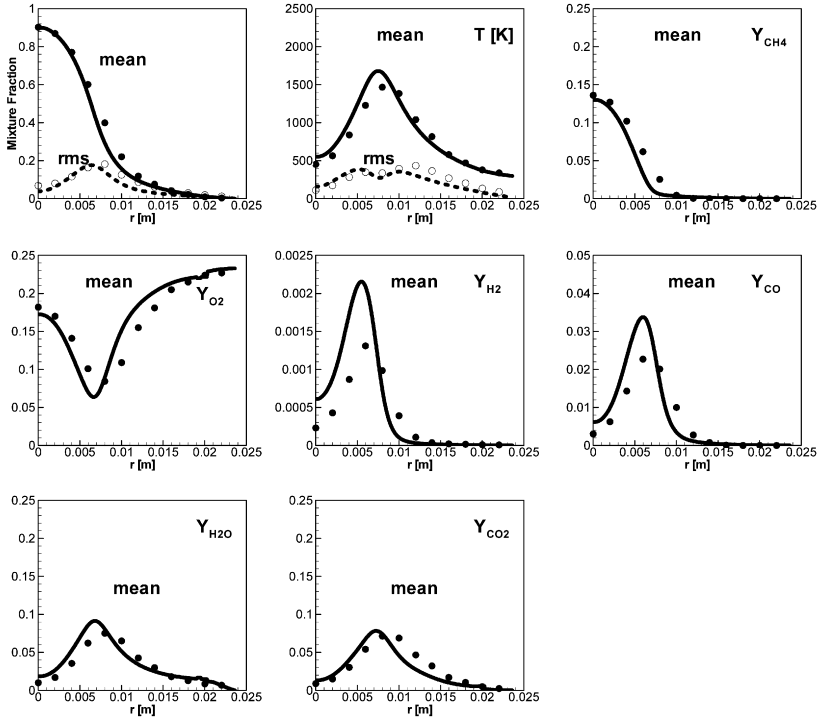

(b)

Fig. 10. Comparison of radial profiles of mixture fraction and reactive scalars from simulations and experiments for flames (a) D, (b) E, and (c) F, at 30 jet diameters. The symbols represent experiments and lines simulations.

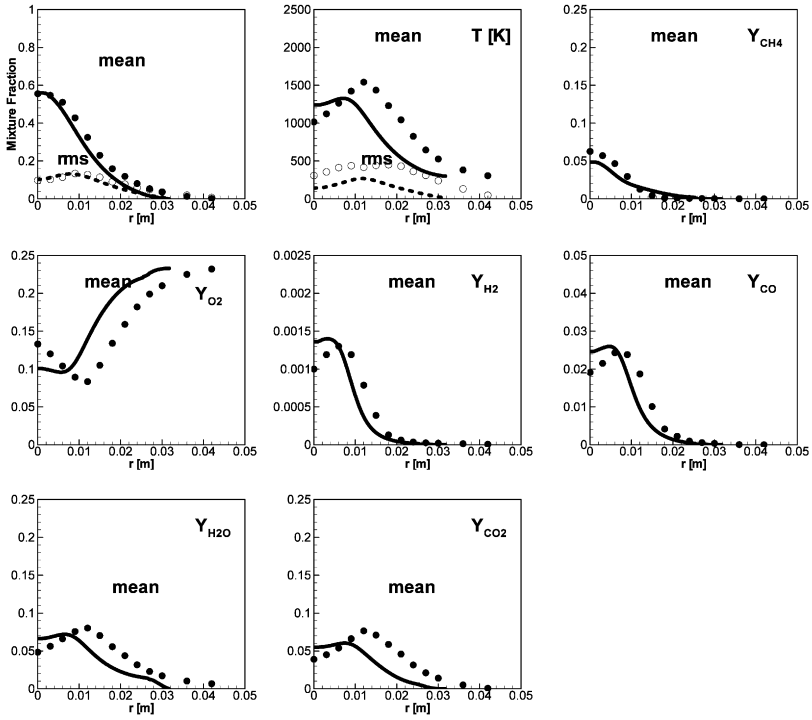

(c)

Fig. 10. (*continued*)

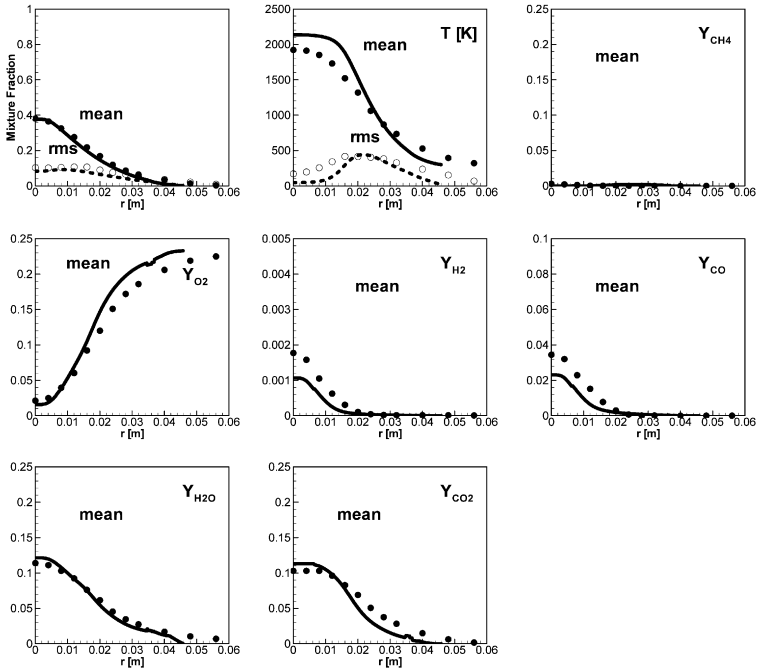

(a)

Fig. 11. Comparison of radial profiles of mixture fraction and reactive scalars from simulations and experiments for flames (a) D, (b) E, and (c) F, at 45 jet diameters. The symbols represent experiments and lines simulations.

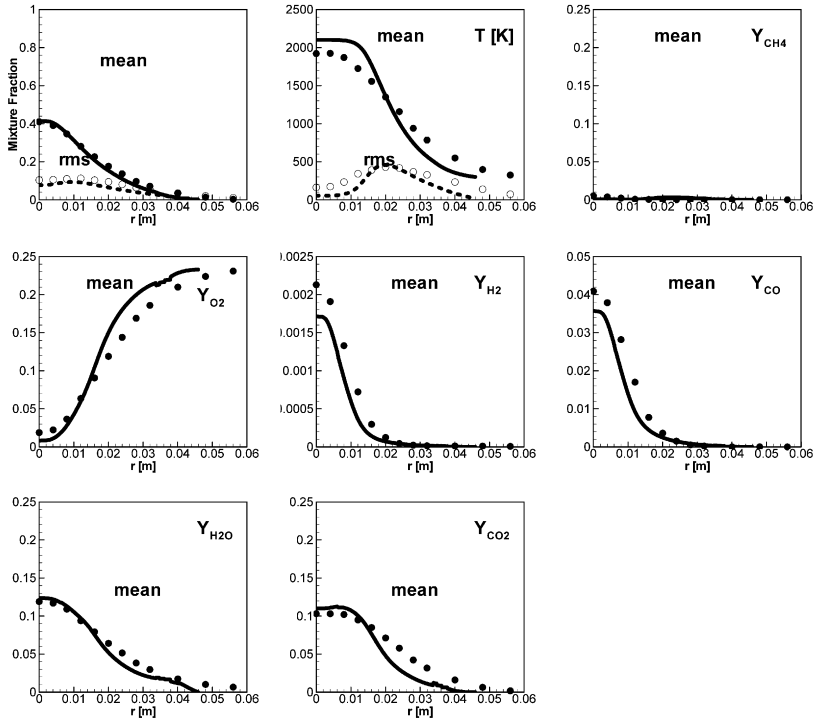

(b)

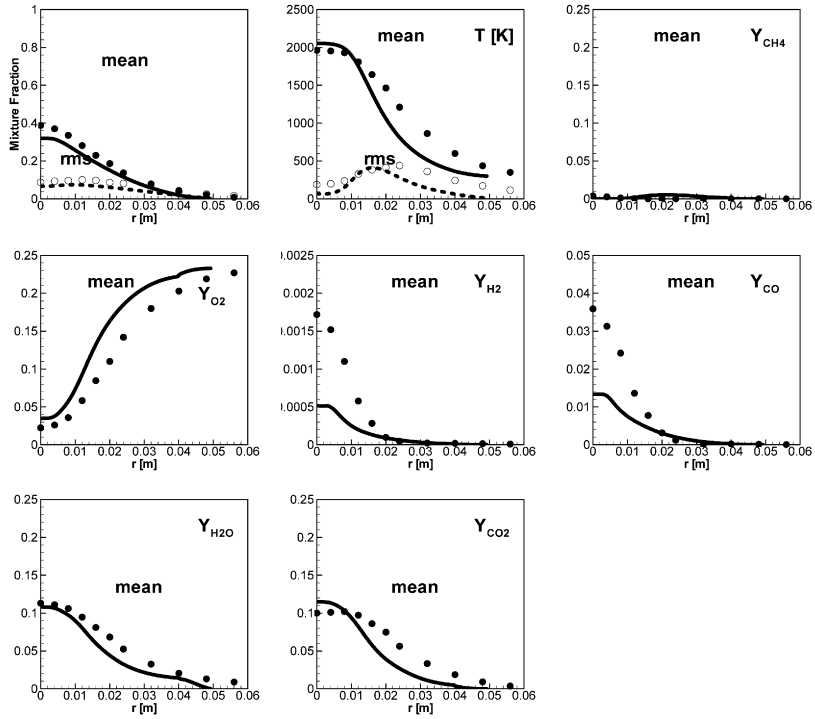

(c)

Fig. 11. (*continued*)

Fig. 11 shows radial profiles of velocity, mixture fraction, temperature, and species mass fractions at $x/d = 45$. At this downstream distance, the experiments have completely recovered from their partially extinguished state. At this axial location, there is good agreement between the experiments and computations as shown with the profiles of the reactive scalars in both flames D and E. In flame F, intermediate species, H_2 and CO, mass fractions are underpredicted approximately by a factor of 3, while the remaining species mass fractions (reactants and products) are reasonably predicted for flame F. The difference between computed and measured means of the mass fractions of intermediates in flame F may be associated again with the predictions of the temperature variance near the axis. The relatively low temperature variance in the computed results near the axis yields equilibrium values for the intermediates.

Based on the above observations, it is evident that uncertainty about closure models for the mean temperature and its variance, as well as the temperature PDF shape, contributes to the spatial profiles of reactive scalars. The computation consistently exhibited a delayed onset of extinction, and the discrepancy between experiment and computation is more prominent at higher Reynolds numbers. The prediction of reactants and major products (H_2O and CO_2) appears to be largely tied to the quality of the prediction of the mean temperature. However, intermediate species exhibits a greater sensitivity to the differences between measured and computed temperature profiles and its variances. Here, the assumed temperature PDF shape is very important because of the strong variations of intermediate species concentrations to variations in Z and T. Past the reignition stage (for example, at $x/d = 45$), the predictions for the computed temperature variances are lower than the measured values. Accordingly, important differences between computed and measured intermediate species profiles are obtained, especially in flame F.

4. Conclusions

The present results illustrate some key observations related to the use of ODT as a generalized flame library to predict extinction and reignition in jet diffusion flames:

- Scalar statistics, conditioned on the mixture fraction and temperature, are essentially the same for shared regions of the conditioning variables regardless of the Reynolds number. This observation is made for the experimental data, but it is equally found in the various conditions run in ODT (not shown in detail here). This observation provides an alternative validation tool for other moment-based approaches.
- Scalar statistics conditional upon the Z and T based on ODT are in excellent agreement with the experimental results. This observation suggests that ODT solutions may be used to generate generalized flame libraries for scalar statistics in reduced-parameter space. A principal advantage of the proposed model over other flamelet-based tabulation approaches is that double conditioning based on Z and T can be implemented based on the same data set with an account of the coupling of molecular processes and turbulent transport under transient conditions. Again, we have not found any fundamental difference between conditions run under the different turbulence conditions or ODT model parameters used.

However, the prediction of spatial profiles of reactive scalars based on the present moment-based modeling approach must equally address closure in the transport equation for temperature and its variance and the corresponding assumed shape PDF. All of these elements appear to contribute at different degrees during the extinction and reignition stages. While reasonable agreement between computation and experiment is found for flames D and E, important discrepancies between the two sets of data are found for flame F. Variants of the closure terms, which correspond to the turbulent transport and source and sink terms for the temperature variance and the turbulent transport for the mean temperature will be explored in the future to assess the model sensitivity to these terms and the associated model constants. With regards to the temperature PDF, strategies to define different PDF shapes based on means and variances for the temperature will be explored since the β-PDF model shape is not adequate for reactive scalars in the presence of extinction. Issues of relevance to the above closure problems are common among the different moment-based approaches. An alternative strategy to the present approach, which is presently explored, is to construct temperature PDFs from the ODT solutions. A similar approach has already been implemented by Goldin [15] and Goldin and Raman [16] using the LEM approach. Important trade-offs between the two strategies are present. In the present approach, the 2D table may be implemented for a wide range of flame conditions, and potentially similar flame/flow configurations (e.g., shear layer, jet in a cross flow) may be computed with the same 2D table. A different set of challenges arise with the strategy of constructed PDFs; among them is the challenge of defining a set of parameters that describe these PDFs. In either strategy, the main ODT advan-

tage is the ability to address important nonequilibrium effects associated with combustion chemistry.

Acknowledgments

This work was supported by a grant from the Air Force Office of Scientific Research. We are grateful to Dr. A. Dreizler for providing us the velocity data for Flames D and F and to Drs. R.S. Barlow and J.F. Frank for providing the scalar data through the TNF workshop Web site.

References

[1] N. Peters, Turbulent Combustion, Cambridge Univ. Press, Cambridge, UK, 2000.
[2] N. Peters, Proc. Combust. Inst. 21 (1988) 1231.
[3] A.Y. Klimenko, R.W. Bilger, Prog. Energy Combust. Sci. 25 (1999) 595.
[4] P. Sripakagorn, S. Mitarai, G. Kosály, H. Pitsch, J. Fluid Mech. 518 (2004) 231–259.
[5] C.M. Cha, G. Kosály, H. Pitsch, Phys. Fluids 13 (2001) 3824–3834.
[6] C.M. Cha, H. Pitsch, Combust. Theor. Model. 6 (2002) 425–437.
[7] A. Kronenberg, Phys. Fluids 16 (2003) 2640–2648.
[8] A. Kronenberg, M. Kostka, Combust. Flame 143 (2005) 342–356.
[9] M. Ihme, C.M. Cha, H. Pitsch, Proc. Combust. Inst. 30 (2005) 793–800.
[10] R.S. Barlow, J.H. Frank, Proc. Combust. Inst. 27 (1998) 1087–1095.
[11] A.R. Kerstein, Combust. Flame 75 (1989) 397–413.
[12] A.R. Kerstein, J. Fluid Mech. 216 (1990) 411–435.
[13] A.R. Kerstein, J. Fluid Mech. 231 (1991) 361–394.
[14] A.R. Kerstein, J. Fluid Mech. 392 (1999) 277–334.
[15] G.M. Goldin, Proc. Combust. Inst. 30 (2005) 785–792.
[16] G.M. Goldin, V. Raman, Proc. Summer Program 2004, Center for Turbulence Research, Stanford University-NASA Ames, pp. 295–304.
[17] J.C. Hewson, A.R. Kerstein, Combust. Theor. Model. 5 (2002) 669–697.
[18] J.C. Hewson, A.R. Kerstein, Combust. Sci. Technol. 174 (2002) 35–66.
[19] B. Ranganath, T. Echekki, Prog. Comput. Fluid Dynam. 6 (2006) 408–418.
[20] T. Echekki, A.R. Kerstein, T.D. Dreeben, J.Y. Chen, Combust. Flame 125 (2001) 1083–1105.
[21] W. Meier, A.O. Vyrodov, V. Bergmann, W. Stricker, Appl. Phys. B Lasers Opt. 63 (1996) 79–90.
[22] M.M. Tacke, S. Linow, S. Geiss, E.P. Hassel, J. Janicka, J.Y. Chen, Proc. Combust. Inst. 27 (1998) 1139–1148.
[23] W.P. Jones, J.H. Whitelaw, Combust. Flame 48 (1982) 1–26.
[24] M. Rullaud, Ph.D. thesis, INSA-Rouen, France (2004).
[25] D. Bradley, D.R. Emerson, P.H. Gaskell, X. Ju, Proc. Combust. Inst. 29 (2002) 2155–2162.
[26] L. Vervisch, R. Hauguel, P. Domingo, M. Rullaud, J. Turb. 5 (4) (2004) 1–36.
[27] C.H. Schneider, A. Dreizler, J. Janicka, E.P. Hassel, Combust. Flame 135 (2003) 185–190.
[28] C.J. Sung, C.K. Law, J.Y. Chen, Combust. Flame 125 (2001) 906–919.
[29] H. Akima, Commun. Am. Chem. Soc. 17 (1) (1974) 18–20.
[30] H. Pitsch, H. Steiner, Phys. Fluids 12 (2000) 2541–2554.
[31] R. Cao, S.B. Pope, Combust. Flame 143 (2005) 450–470.